Machine vision based expert system to estimate orange mass of three varieties

Hossein Javadikia*, Sajad Sabzi, Hekmat Rabbani

(*Department of Mechanical Engineering of Biosystems, Faculty of Agriculture, College of Agriculture and Natural Resources, Razi University, Kermanshah, 67156-85438, Iran*)

Abstract: A key issue in fruit export is classification and sorting for acceptable marketing. In the present work, the image processing technique was employed to grade three varieties of oranges (Bam, Khooni and Thompson) separately. The reason for choosing this fruit as the object of the study was its abundant consumption worldwide. In this study, 14 parameters were extracted: area, eccentricity, perimeter, length/area, blue value, green value, red value, width, contrast, texture, width/area, width/length, roughness, and length. Further, the ANFIS (Adaptive Network-based Fuzzy Inference System) method was utilized to estimate the orange mass from the data obtained using the image processing in three varieties. In ANFIS model, samples were divided into two sets, one with 70% for training set and the other one with 30% for testing set. The results of the present study demonstrated that the coefficient of determination (R^2) of the best model for Bam, Khooni and Thompson measured 0.948, 0.99, and 0.98, respectively. In addition, the results indicated that the estimation accuracy of the best model for Bam, Khooni and Thompson was measured as ±3.7 g, ±1.28 g, ±3.2 g, respectively. This result was very satisfactory for the application of ANFIS to estimate the orange mass.

Keywords: ANFIS, orange, machine vision, mass, sorting
DOI: 10.3965/j.ijabe.20171002.1737

Citation: Javadikia H, Sabzi S, Rabbani H. Machine vision based expert system to estimate orange mass of three varieties. Int J Agric & Biol Eng, 2017; 10(2): 132–139.

1 Introduction

According to the published statistics, Iran is known as the sixth citrus producers around the world[1]. So, the old methods of sorting must be replaced by new ones in Iran to have standard packaging and ability of challenge in world marketing. A machine vision system provides grading ability without the human intervention. The artificial intelligence techniques are proper methods in data analysis almost[2]. So, using one of the artificial intelligence methods and image processing, a fully automated grading system with a low percentage error can be proposed. The grading system has the benefits of high grading speed and accuracy with low labor cost. The applications of machine vision in agriculture have been reported by some scholars. Mizushima et al.[3] studied the postharvest citrus mass and size estimation using a logistic classification model and a watershed algorithm. The highest coefficient of determination (R^2) value between the measured fruit mass and the estimated fruit mass was 0.945 and the root mean square error measured 116.1 kg. Tong et al.[4] applied the machine vision to estimate the quality of seeds of tomato, cucumber, aborigine and pepper based on the areas of leaves. Both a decision method and a methodology were improved to watershed the segmentation for the overlapping leaf (OL) images. The relative identification accuracy values for the seedling quality

Received date: 2015-02-18 **Accepted date:** 2016-11-08
Biographies: Sajad Sabzi, MS, Lecturer, research interests: image processing and artificial intelligence in agriculture, Email: sajadsabzi2@gmail.com; **Hekmat Rabbani:** PhD, Associate Professor, research interest: mechanical engineering of agricultural machinery, Email: hrabbani47@razi.ac.ir.

***Corresponding author: Hossein Javadikia**, PhD, Assistant Professor, research interest: image processing and artificial intelligence in agriculture. Razi University, Kermanshah, 67156-85438, Iran. Tel: +98-831-8331662, Mobile: +98-914-3149289; Email: pjavadikia@gmail.com, h.javadikia@razi.ac.ir.

measured 98.6%, 96.4%, 98.6% and 95.2% for tomato, cucumber, aborigine and pepper, respectively. Li et al.[5] used the machine vision system for the identification of micro-cracks in egg shells. They exploited a chamber with a vacuum pressure of 18 kPa to open the crack. The system could identify the cracked and intact eggs with 100% accuracy. Pandey et al.[6] investigated the application of a method to automatically detect the common surface defects on oranges through the combined lighting transform and image ratio methods. The results showed that this method could not differentiate between different types of defects on the skin of orange, but it could differentiate between the normal and defective oranges. Shin et al.[7] utilized an android mobile phone to estimate the citrus yield based on image processing. The results indicated that there was a satisfactory average estimation ratio (90%) between the actual and predicted fruit yields. An image segmentation method was proposed for apple sorting and grading using the support vector machine and Otsu's method[8]. The segmentation error was less than 2%. Xu et al.[9] used a method for the automatic classification of non-touching cereal grains, namely barley, oat, rye and wheat (Canada Western Amber Durum (CWAD) and Canada Western Red Spring (CWRS)) in digital images using the limited morphological and color features. The combined model, defined by the morphological and color features, achieved a classification accuracy of 98.5% for barley, 99.97% for CWRS, 99.93% for oat, and 100% for rye and CWAD. Other studies were also conducted in this respect such as[10-18].

One of the goals of volume or mass sorting was putting relatively identical fruits in a packages, thereby resulting in minimizing losses in transportation. Since the orange size is more related to its mass, the mass-based sorting system was considered in the present study. The sorting operation should be done automatically to boost accuracy, time saving and performance. Image processing is coupled with an artificial intelligence method named ANFIS to achieve these aims. Such a methodology is novel and there exists no report in this regard in the literature. Therefore, the idea behind this research is original.

2 Materials and methods

In this study, three varieties of orange, namely Bam, Khooni and Thompson were used (see Figure 1). Since the size of the orange population was more than 100 000, one hundred of each variety of orange was selected as the sample size[19]. Samples were bought from north of Iran (center of citrus cultivation in Iran) and were transported into the laboratory of biophysical and mechanical properties of agricultural materials in Razi university of Kermanshah in Iran. All of the experiments such as the measurement of mass and extract of physical properties of oranges were done in one day. Mass of oranges was measured with a digital balance with an accuracy of ±0.1 g.

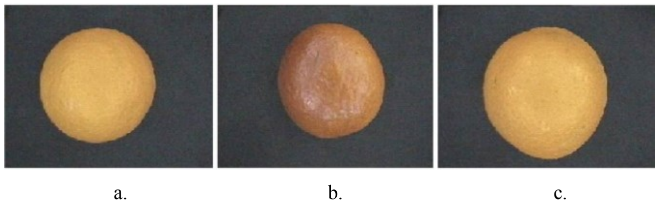

Figure 1 The Photographs of (a) Bam orange, (b) Khooni orange, and (c) Thompson orange

2.1 Image processing

A machine vision system was developed towards image acquisition. The proposed system consisted of an image acquisition system (see Figure 2), a digital camera (BOSCH, made in Germany), a frame grabber (made in China) and a personal computer (PC) equipped with MATLAB (Version R2009b) and Microsoft excel (Version 2010) programs. Images were provided with a resolution of 352×288 pixels by a digital camera. It was mounted 10 cm above the sample. Three types of lamps (LED, fluorescent and tungsten) were provided around the sample to remove any shadow in the image acquisition process.

In this study, the fluorescent lamps with light intensity of 50.33 lx were used. The images were captured from fruit samples and were transferred to the PC through the video capture card. The images were digitized and stored into four user-defined buffers in red, green and blue color coordinates (RGB) and gray scale for further analysis. The black cardboard was used as the background surface to do the segmentation task. A computer program was written in MATLAB (Version R2009b) and developed for processing and analyzing the captured images. Additionally, fourteen parameters were extracted from images: area, eccentricity, perimeter, length/area, blue value, green value, red value, width, contrast, texture, width/area, width/length, roughness, length. Further, the seven methods of Sobel, Prewitt, Roberts, Laplacian of Gaussian, zero-cross, Canny and F special function with Sobel type were used to detect. The Sobel, Prewitt and Roberts's methods find the edge using the Sobel Prewitt and Roberts approximations to the derivative. They return the edge at those points where the gradient is high. The Laplacian of Gaussian method finds the edge by looking for zero crossing after filtering. The Canny method finds the edge through looking for the local maximization of the gradient. The gradient is calculated using the derivative of a Gaussian filter.

Note: 1. Tungsten 2. Camera carrier (Frame grabber) 3. Camera 4. LED 5. Fluorescent

Figure 2 The special chambers for image acquisition

Two thresholds were applied to detect the strong or weak edges in this method. This method is therefore less likely than other methods to be wrong by noise and more likely to detect truly weak edges. $H = F$ special ('Sobel') returns a 3×3 Mask H (Equation (1)) that emphasizes the horizontal edge using the smoothing effect by approximating a vertical gradient. If the vertical edge needs emphasis, Equation (2) can be used to transpose the filter H'.

$$H = \begin{bmatrix} 1 & 2 & 1 \\ 0 & 0 & 0 \\ -1 & -2 & -1 \end{bmatrix} \tag{1}$$

$$H' = \begin{bmatrix} 1 & 0 & 1 \\ 2 & 0 & -2 \\ -1 & 0 & -1 \end{bmatrix} \tag{2}$$

Equation (3) must be used to detect the edge with $h = F$ special ('Sobel').

$$h = \sqrt{H^2 + H'^2} \tag{3}$$

where, 'H' is the horizontal edge and 'H' is the vertical edge[20].

2.2 Application of ANFIS

ANFIS is a fuzzy Sugeno model placed in the frame of adaptive systems to expedite learning and adaptation[21]. To identify the membership function parameters and fuzzy if–then rules based on one output singleton, the Sugeno type fuzzy inference systems (FIS) applies a combination of least-squares and back propagation gradient descent methods along with a hybrid learning algorithm. The singleton fuzzy systems can be simplified by the restriction to singleton output membership functions in the complex defuzzification phase[21]. The ANFIS structure consists of five layers as shown in Figure 3.

2.3 Statistical analysis

Coefficient of determination (R^2), sum squared error (SSE) and mean squared error (MSE) were used to evaluate the models. It is evident that the model which has the highest value of R^2 and the lowest value of SSE and MSE represents a best estimation. Equations (4) to (7) show R^2, X_m, MSE and SSE formulas, respectively.

$$R^2 = 1 - \left\{ \frac{\sum_{k=1}^{n} (X_s - X_0)^2}{\sum_{k=1}^{n} (X_s - X_m)^2} \right\} \tag{4}$$

$$X_m = \frac{1}{n} \sum_{k=1}^{n} X_s \tag{5}$$

$$\mathrm{MSE} = \frac{1}{n} \sum_{k=1}^{n} (X_s - X_0)^2 \tag{6}$$

$$\mathrm{SSE} = \sum_{k=1}^{n} (X_s - \overline{X_0})^2 \tag{7}$$

where, X_s is the actual values; X_0 is the forecasted values; $\overline{X_0}$ is the average of experimental values; X_m is the mean of the actual values and n is the number of forecasts. These parameters evaluate the agreement between the actual and forecasted values.

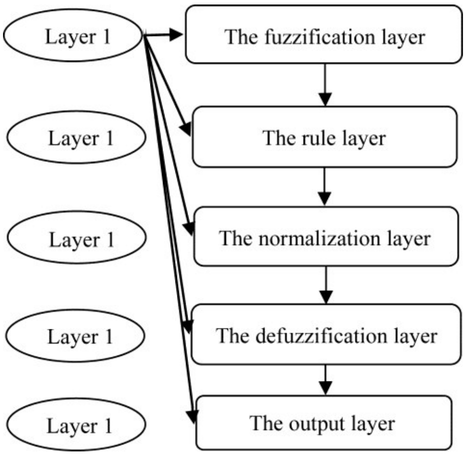

Figure 3 ANFIS framework

3 Results and discussion

3.1 RGB images

The images which were captured from samples must be converted to three components: red, green and blue to determine the best conditions for separating the fruits from background. The red, green and blue images are shown in Figure 4. Figure 4 also shows that the numbers of red pixels are abundant in three varieties. So, Figures 4a, 4d and 4g are the brightest images. Figure 5 shows the histograms of red, green and blue images. In these histograms, the difference between the left and right pikes shows which image is good for extracting data from oranges. The left pike is related to the pixels of the background color, and the right pike is related to the pixels of the fruit color. If the difference is big, it is easy to separate. Figure 5 shows that the difference of the two pikes is farthest in the red image in each variety. Hence, it was necessary to convert the captured images to red ones to do other operations on images.

3.2 Edge detection

The edge of samples was detected to get the texture and roughness. Figure 6 shows the results of seven methods for edge detecting. Figure 6 is divided into three parts. The first part (from 'a' to 'g') is related to Khooni orange, the second part (from 'h' to 'n') is related to Thompson orange, and the third part (from 'o' to 'v') is related to Bam orange. In each of the three varieties, these images are related to Canny, Laplacian of Gaussian, Prewitt, Roberts, F special function with Sobel type, Sobel and zero-cross methods, respectively. All methods with Sobel type had good results for Khooni orange except for the F special function. The reason of this problem refers to filter H (Equation (1)). In this image, the result of multiplying each pixel in its equivalent member in filter H due to similar values of pixels in these areas and sum of them was zero. So, boundaries of these areas could not be obtained. Three methods of Canny, Laplacian of Gaussian and zero-cross did not have good results for Thompson and Bam oranges. The Canny method was used for local maximum to find the edges. If the local maximums are similar in other areas, the edge will cause the error.

In the Laplacian of Gaussian method, the edge is recognized by finding the zero crossing between two limitations that are recognized with Laplacian filter. If the Laplacian filter has errors in recognizing two limitations due to noise, other points are selected as the edge erroneously. The zero-cross method acts the same as the Laplacian of Gaussian method.

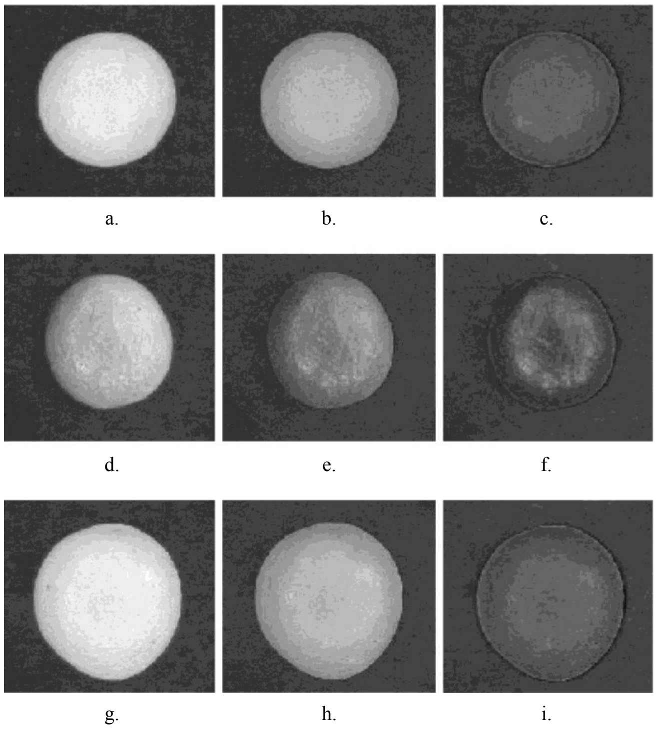

Figure 4 The component of image: (a), (b), (c) are the red, green, blue images of Bam orange, respectively. (d), (e), (f) are the red, green, blue images of Khooni orange, respectively. (g), (h), (I) are the red, green, blue images of Thompson orange, respectively

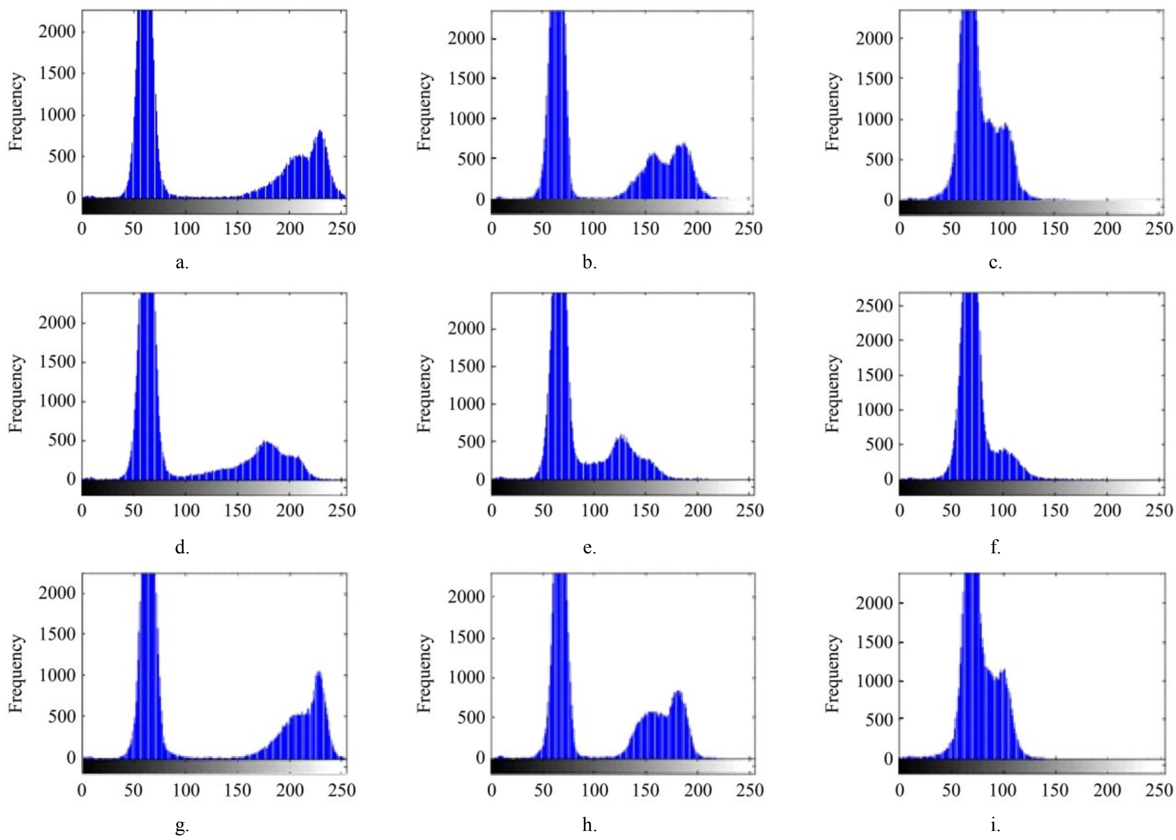

Figure 5 The histogram of image: (a)-(c) red, green, blue image of Bam orange, respectively. (d)-(f) are the red, green, blue images of Khooni orange, respectively. (g)-(I) are the red, green, blue images of Thompson orange, respectively

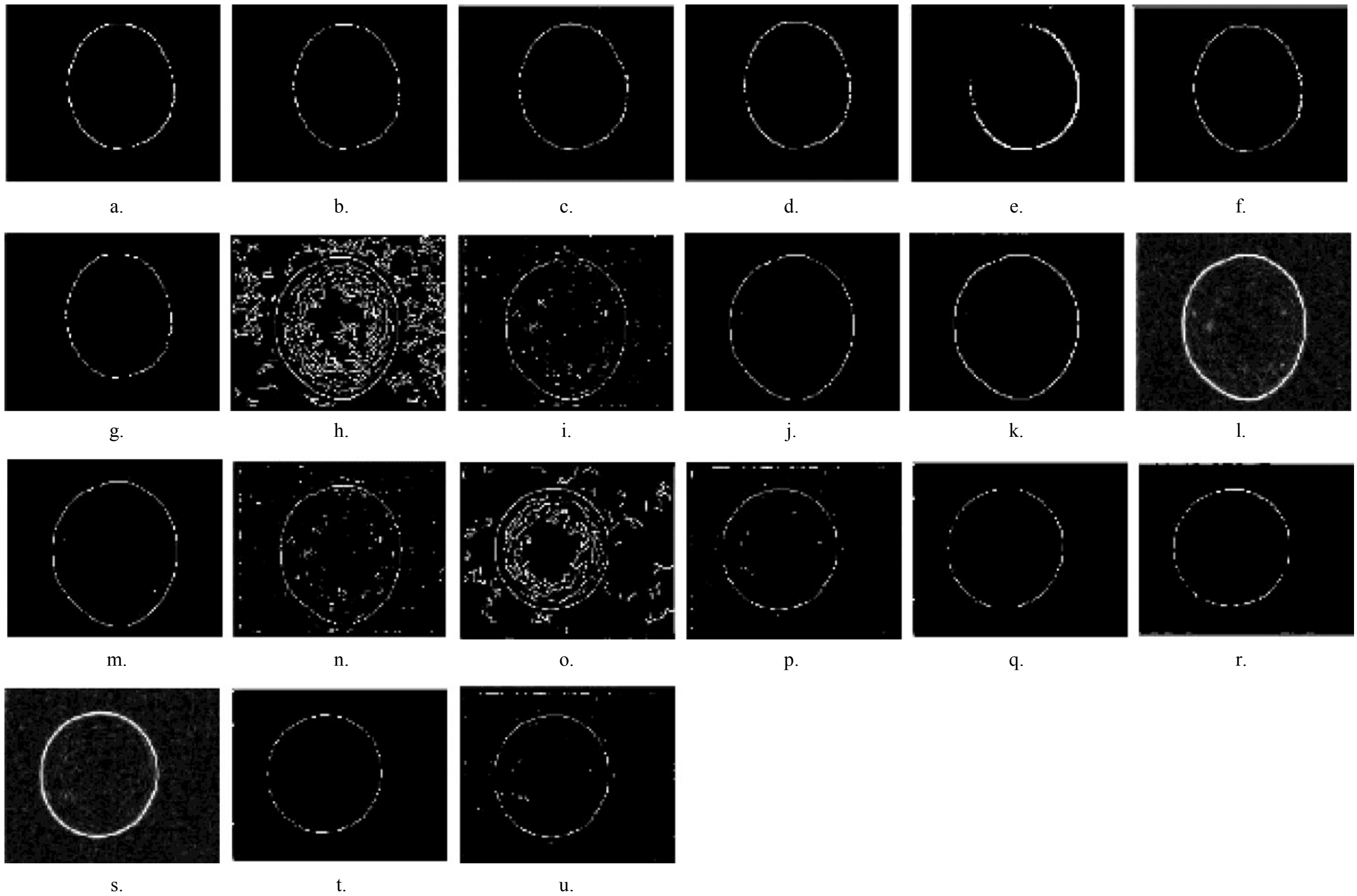

Figure 6 Edge detection methods: (a) Canny, (b) Laplacian of Gaussian, (c) Prewitt, (d) Roberts, (e) F special function with Sobel type, (f) Sobel and (g) zero-cross, respectively for khooni orange, from (h)-(n) and (o)-(u) with the same order are for Thompson and Bam oranges, respectively

3.3 ANFIS results

The ANFIS method was applied to determine the mass of oranges with inputs obtained through the image processing algorithm. Several models were presented for orange mass based on ANFIS in Tables 1-3 for Bam, Khooni and Thompson varieties, respectively. The models were compared with three parameters R^2, SSE and MSE. Five different adjustments must be made to the ANFIS method to construct models, namely: the membership function type for input, the number of membership functions for input, the membership function type for output, the optimization method and the number of epochs. The model has acceptable results when these adjustments are made accurately.

In Table 1, the models with two or three inputs have better results than the ones with one input. If one input is used for model, the prediction of the output solely depends on this input, but if two or more inputs are used, the prediction of the output hinges on the combination of inputs. So, if one of the inputs is noisy, the models with several inputs have fewer errors than that with one input.

In Tables 2 and 3, it can be seen that the models with inputs with texture features (texture and roughness) have worse results than the ones with inputs with dimensional features (length, width, area and perimeter). Furthermore, the texture feature was used in the models since its effects were considered on the orange mass. It seems that the type of the orange peel may affect the mass. Finally, the models showed that it was not effective.

In the ANFIS model, the effects of the input parameters on the output can be illustrated through the graphical representation of visual perception[22].

For this purpose, the variation of the mass of Bam is plotted against (a) width, contrast (b) width, and area (see Figure 7). It can be seen in Figure 7a that the mass has maximum values in line with any increase in the area. Figure 7b shows that mass value increases proportional to the width.

Table 1 Summary of properties from some ANFIS models for Bam orange with different inputs

No	MF input	MF number	Epoch number	MF output	Input 1	Input 2	Input 3	R^2	SSE	MSE
1	trimf	2 2	3	constant	width/length	perimeter	-	0.948	405.7	13.99
2	trimf	2 2 2	10	linear	roughness	green value	area	0.935	585.4	19.51
3	gaussmf	2 2	1000	constant	length	area	-	0.912	759.8	25.33
4	gaussmf	3 3	100	linear	length/area	width /area	-	0.819	834.3	27.81
5	trimf	2	100	constant	width	-	-	0.779	728.7	24.29
6	trimf	2	150	linear	length	-	-	0.323	2.685	0.0268
7	trimf	3	250	constant	area	-	-	0.044	1.443	0.048

Table 2 Summary of some models for khooni orange based on ANFIS model with different inputs

No	MF input	MF number	Epoch number	MF output	Input 1	Input 2	Input 3	R^2	SSE	MSE
1	gbellmf	3 3 3	120	constant	area	perimeter	green value	0.99	21.5	1.65
2	trimf	2 2	1000	constant	area	perimeter	-	0.94	318.9	2.58
3	trimf	2 2	120	linear	length	width	-	0.95	282.9	2.34
4	dsigmf	5 5 5	250	constant	length	width	contrast	0.91	449.3	2.77
5	trimf	2 2 2	20	constant	texture	contrast	roughness	0.91	368.9	2.76
6	Gausa2mf	2 2 2	10	linear	width/area	length/area	width/length	0.89	379.2	2.89

Table 3 Summary of properties from some of ANFIS models for Thompson orange with different inputs

No	MF input	MF number	Epoch number	MF output	Input 1	Input 2	Input 3	R^2	SSE	MSE
1	gbellmf	3 3 3	70	constant	length	width	area	0.98	314.99	10.49
2	gbellmf	3 3 3	92	constant	red value	green value	blue value	0.9	115.85	3.86
3	psigmf	3 3 3	110	constant	length	red value	area	0.8	3394.9	113.16
4	psigmf	3 3 3	65	linear	texture	contrast	roughness	0.557	27189	906303
5	gauss2mf	3 3 3	100	constant	area	roughness	contrast	0.471	13693	456.46
6	dsigmf	3 3 3	125	constant	area	red value	green value	0.032	51052	1701.75

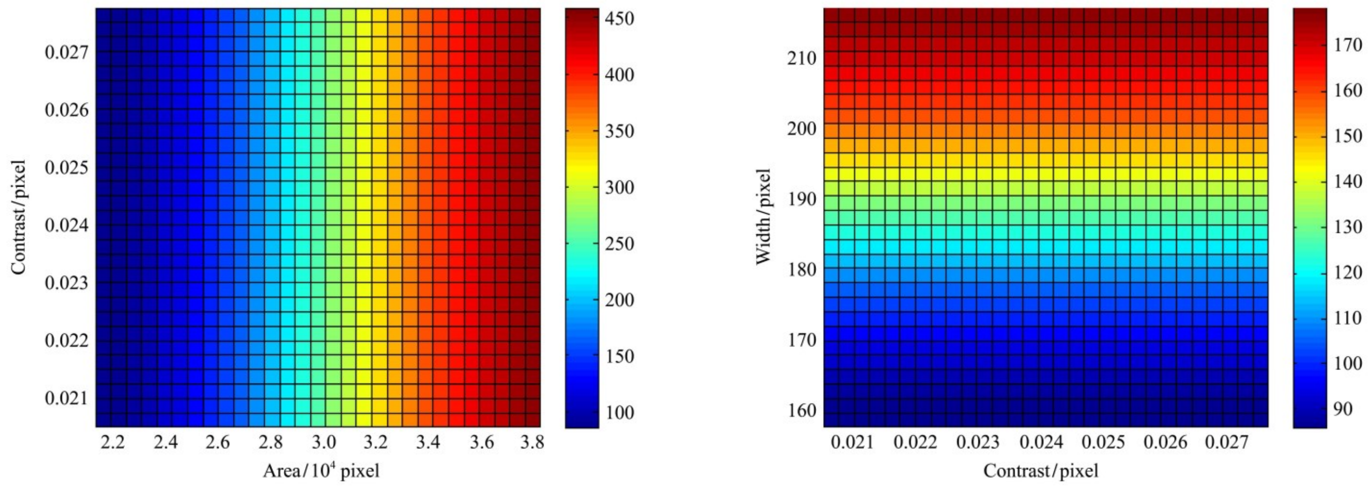

a. Contrast-Area b. Width-Contrast

Figure 7 Mosaic mapping for volume modeling of Bam orange

3.4 Grading system proposal

The grading system is shown in Figure 8. The oranges with different sizes are placed on the conveyor belt and the camera takes images from them. Then the images are transferred to the computer for analysis with the help of an algorithm developed in MATLAB. After analysis, fruits are divided into three groups: small, medium, and large. Three lines are built to transmit the oranges with different sizes: small, medium, and large toward the packaging sector.

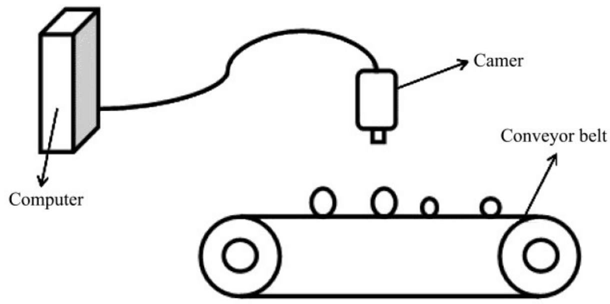

Figure 8 Layout of computer mediated fruit sorting system

4 Conclusions

In this paper, the ANFIS method along with a strong algorithm written in MATLAB Software were employed to explore the prediction techniques for the mass modeling of three varieties of oranges (Bam, Khooni, and Thompson) based on fourteen features. The results of the present study demonstrated that the coefficient of determination (R^2) of the best model for Bam, Khooni and Thompson measured 0.948, 0.99, 0.98, respectively. In addition, the results indicated that the estimation accuracy of the best model for Bam, Khooni and Thompson was measured as ±3.7 g, ±1.28 g, ±3.2 g, respectively. The proposed grading system in this study can be utilized in the grading industry.

Acknowledgment

The authors would like to acknowledge the financial support from Razi University and Ministry of Science, Research and Technology of Iran.

[References]

[1] Adelkhani A, Beheshti B, Minaei S, Javadikia P, Ghasemi-Varnamkhasti M. Taste characterization of orange using image processing combined with ANFIS. Measurement, 2013; 46: 3573–3580.

[2] Li J, Rao X, Wang F, Wu W, Ying Y. Automatic detection of common surface defects on oranges using combined lighting transform and image ratio methods. Postharvest Biology and Technology, 2013; 82: 59–69.

[3] Mizushima A, Lu R. An image segmentation method for apple sorting and grading using support vector machine and Otsu's method. Computers and Electronics in Agriculture, 2013; 94: 29–37.

[4] Tong J H, Li J B, Jiang H Y. Machine vision techniques for the evaluation of seedling quality based on leaf area. Biosystems Engineering, 2013; 115: 369–379.

[5] Li Y Y, Dhakal S, Peng Y K. A machine vision system for identification of micro-crack in egg shell. Journal of Food Engineering, 2012; 109: 127–134.

[6] Pandey R, Naik S, Marfatia R. Image processing and machine learning for automated fruit grading system: A

technical review. International Journal of Computer Applications, 2013; 81(16): 29–39.

[7] Shin J S, Lee W S, Ehsani R. Postharvest citrus mass and size estimation using a logistic classification model and a watershed algorithm. Biosystems Engineering, 2012; 113: 42–53.

[8] Ho C, Tsai T. Comparing ANFIS and SEM in linear and nonlinear forecasting of new product development performance. Expert Systems with Applications, 2011; 38: 6498–6507.

[9] Xu L M, Zhao Y C. Automated strawberry grading system based on image processing. Computers and Electronics in Agriculture, 2010; 71: 32–39.

[10] Wang Q H, Tang Y H, Xiao Z. Grape size detection and online gradation based on machine vision. Int J Agric & Biol Eng, 2017; 10(1): 226–233.

[11] Gong A, Yu J, He Y, Qiu Z. Citrus yield estimation based on images processed by an Android mobile phone. Biosystems Engineering, 2013; 115: 162–170.

[12] Wang J L, Han Y, Zhao S S, Zheng H X, He C, Cui X Y, et al. A new multi-scale analytic algorithm for edge extraction of strawberry leaf images in natural light. Int J Agric & Biol Eng, 2016; 9(1): 99–108.

[13] Nagle M, Intani K, Romano G, Mahayothee B, Sardsud V, Müller J. Determination of surface color of ‘all yellow’ mango cultivars using computer vision. Int J Agric & Biol Eng, 2016; 9(1): 42–50.

[14] Javadikia P, Dehrouyeh M.H, Naderloo L, Rabbani H, Lorestani A N. Measuring the weight of egg with image processing and ANFIS model. Lecture Notes in Computer Science, 2011; 7076: 407–416.

[15] Fu L S, Wang B, Cui Y J, Su S, Gejima Y, Kobayashi T. Kiwifruit recognition at nighttime using artificial lighting based on machine vision. Int J Agric & Biol Eng, 2015; 8(4): 52–59.

[16] Xu K R, Lu X, Wang Q H, Ma M H. Online automatic grading of salted eggs based on machine vision. Int J Agric & Biol Eng, 2015; 8(1): 35–41.

[17] Sabzi S, Javadikia P, Rabbani H, Adelkhani A, Naderloo L. Exploring the best model for sorting blood orange using ANFIS method. Agricultural Engineering International: CIGR Journal, 2013; 15(4): 213–219.

[18] Sabzi S, Javadikia P, Rabbani H, Adelkhani A, Mass modeling of Bam orange with ANFIS and SPSS methods for using in machine vision. Measurement, 2013; 46(9): 3333–3341.

[19] Yamane T. Statistics: An Introductory Analysis, 2nd Ed., New York: Harper and Row, 1967.

[20] Naderloo L, Alimardani R, Omid M, Sarmadian F, Javadikia P, Torabi M Y, et al. Application of ANFIS to predict crop yield based on different energy inputs. Measurement, 2012; 45: 1406–1413.

[21] Ercisli S, Sayinci B, Kara M, Yildiz C, Ozturk I. Determination of size and shape features of walnut (*Juglans regia* L.) cultivars using image processing. Scientia Horticulturae, 2012; 133: 47–55.

[22] Cabalar A F, Cevik A, Gokceoglu C. Some applications of Adaptive Neuro-Fuzzy Inference System (ANFIS) in geotechnical engineering. Computers and Geotechnics, 2012; 40: 14–33.